Growth and characterization of bi doped Cu$_2$S nano crystalline thin films

Ali Abdullah H. AL-Hamdani; Bushra K. H. AL-Maiyaly ✉

🔴 Check for updates

CrossMark

🌐 View Online   ➡️ Export Citation

Articles You May Be Interested In

Effect of Ag doping on optical constant and hall effect measurements of SnS thin films

AIP Conference Proceedings (April 2023)

Structure, morphology and optical properties of thermally evaporated Cu$_2$S thin films annealed at different temperatures

AIP Conference Proceedings (August 2019)

Study and preparation of optoelectronic properties of AgAl$_{1-x}$In$_x$Se$_2$/Si heterojunction solar cell applications

AIP Conference Proceedings (August 2022)

AIP Publishing

Growth and Characterization of Bi doped Cu$_2$S Nano Crystalline thin films

Ali Abdullah. H. AL- Hamdani [a] ، Bushra K. H. AL-Maiyaly [b]

Department of physics, College of Education For Pure Science (Ibn Al-Haitham), University of Baghdad, Baghdad, Iraq.

[a] Ali.Abdullah1204a@ihcoedu.uobaghdad.edu.iq
[b] Corresponding author: boshra.k.h@ihcoedu.uobaghdad.edu.iq

Abstract. Nano crystalline copper sulphide (Cu$_2$S) thin films pure and 3% Bi doped were deposited on glass substrate by thermal evaporation technique of thickness 400±20 nm under a vacuum of $\sim 2 \times 10^{-5}$ mbar to study the influence of annealing temperatures (as-deposited, and 573) K on structural, surface morphology and optical properties of (Cu$_2$S and Cu$_2$S:3%Bi). (XRD) X-ray diffraction analysis showed (Cu$_2$S and Cu$_2$S:3%Bi) films before and after annealing are polycrystalline and hexagonal structure. AFM measurement approves that (Cu$_2$S and Cu$_2$S:3%Bi) films were Nano crystalline with grain size of (105.05-158.12) nm. The optical properties exhibits good optical absorption for Cu$_2$S:3%Bi films. Decreased of optical band gap from 2.25 to 2 eV after doping which indicate good films for Photovoltaic application. The optical constants was carried out by range (300-1100) nm wave length.

Keywords: thin films, copper sulphide, Cu$_2$S:3%Bi, thermal evaporation.

INTRODUCTION

Because of their structural, optical, and electrical properties of Cu$_2$S thin films, copper sulphide is regarded as a promising material for solar energy conversion systems, particularly as p-type semiconductors [1 B]. Cu$_2$S thin film research has received a lot of attention in recent years because of its potential in a photovoltaic cell and its numerous technological applications in the achievement of solar cells, tubular solar cells, photovoltaic misdirection's of solar energy [2-9], vehicle glazing, as solar absorption coating, dye-sensitized solar cells, photo analyzer, microwave protective coating coatings, and sensors, and so on. [10-13]. Responsive resonator sputtering [14], alchemy bath precipitation [1,15-18], drizzle thermal decomposition [19], sequential ionic tier adsorption and response [20], microwave support chemical bath deposition [21], thermal evaporation [9], and chemical steam precipitation [22] have all been used to deposit thin films copper sulphide. Thermic vaporization was used to create thin films copper sulfide, and the impact of 3 % Bi doping and then annealing at 573 K on structure and visible characteristics was studied.

EXPERIMENTAL DETAILS

(Cu$_2$S) alloy was created by combining high purity (99.99 percent) copper (Cu) and sulfur (S) elements in a 1:1 atomic weight ratio, then placing it in an evacuated quartz tube that was heated at 1273 K in a thermal furnace for five hours before being allowed to cool to R.T. The tube was removed from the furnace and broken at one end to retrieve the composite ingot, which was then processed in a special mill (laboratory mill) to produce the material's powder. Cu2S thin films were made from powder on glass substrates with R.T of 400 nm thicknesses using a thermal evaporation process in a vacuum of 10-5 mbar, then doped with 3% Bi and heat treated for an hour at 573 K. X–ray diffraction was used to study the structures of Cu$_2$S alloy and all films, both pure and doped, using a (SHIMADZU-Japan-XRD

6000) diffract meter system with CuK radiation. (λ = 1.5418), 20 mA current, 40Kv voltage, and optical measurements have all been performed.

RESULTS AND DISCUSSIONS

X-ray Diffraction Analyses

Figure (1) shows the XRD spectrum of Cu_2S thin films formed by thermal evaporation process with a thickness of 400 nm that are pure and doped 3 % Bi at (R.T and Ta=573 K). All of these XRD patterns demonstrate the polycrystalline nature of the films and the creation of the Cu_2S phase, which is archived in the standard ICDD (00-053-0522) card with peaks at 2= 16.027, 36.33, 45.99, 51.82, and 54.40 matching to (100), (210), (220), (310), and (311) respectively. XRD patterns further demonstrate that all films made have a single phase crystal and are extremely pure, as no secondary phase is found. Furthermore, after doping and annealing (at Ta=573 K), the preferred orientation along the (220) plane increased, peaks were sharper, and crystalline size increased, implying that Nano crystallite size grew.

The size of the crystals is computed using Scherer's formula.[23]:

$$C.S = \frac{0.94\lambda}{\beta cos\theta} \quad \dots\dots\dots\dots\dots\dots(1)$$

The XRD wave length is represented by: λ, The FWHM of the peaks is shown by: β, and Bragg's angle is represented by: θ, To compute the dislocation density (δ), Williamson and Smallman's equation was used [23]:

$$\delta = \frac{1}{(C.S)2} \quad \dots\dots\dots\dots\dots.. (2)$$

Tables (1) and (2), respectively, include all of these values for Cu_2S alloy and films.

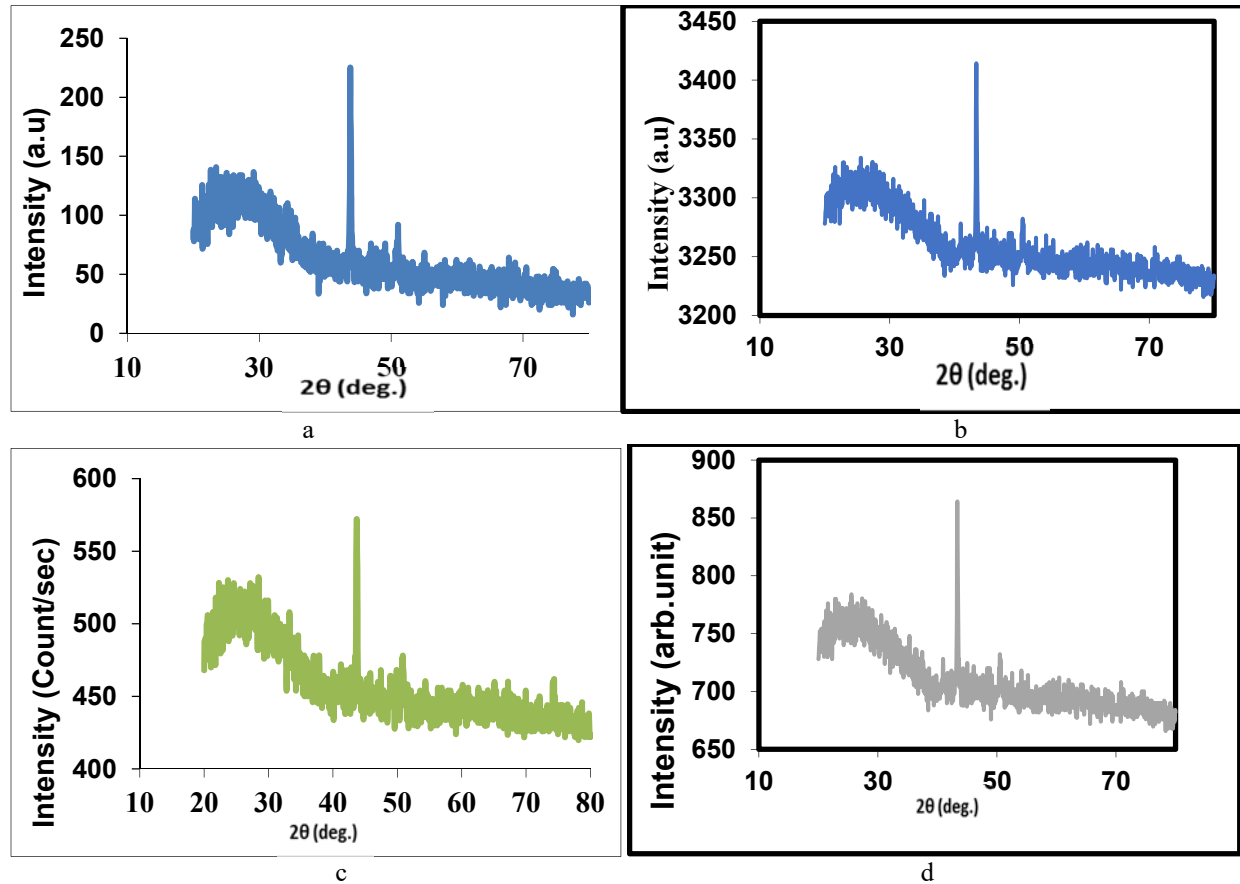FIGURE 1. XRD results for Cu2S thin films a) pure at R.T. b) pure at Ta=573 K c) 3 % Bi doped at (273k) d) 3 % Bi doped at (Ta=573 K)

TABLE 1. Cu₂S alloy structural characteristics.

2θ (Std.) (Deg.)	2θ (Exp.) (Deg.)	d(Std) (Å)	d(Exp) (Å)	hkl	FWHM (Deg.)	C.S (nm)	a(Std.) (Å)	a(Exp.) (Å)
15.9152	16.0272	5.564000	5.52550	100				
36.1076	36.3375	2.485500	2.47036	210				
46.1034	45.9980	1.967200	1.97151	220	0.39570	22.7998	5.564Å	5.570Å
51.9251	51.8274	1.759500	1.76263	310				
54.6724	54.4014	1.677400	1.68516	311				

TABLE 2. Characteristics of Cu₂S films structure.

Sample	T(K)	2θ	FWHM(deg)	d_{hkl} (exp) A°	$d_{hkl (std)}$ A°	C.S (nm)	$\delta * 10^{15}$ (lines/m^2)
Cu₂S	R.T	43.8375	0.21220	2.0723	2.0635	42.1583	0.000562
		51.0178	0.30000	1.7900	1.7886	30.659	0.00107
Cu₂S	573	35.5424	0.5900	2.5257	2.5237	14.7747	0.00458
		38.7098	0.7000	2.3260	2.3242	12.5697	0.006329
Cu₂S:3% Bi	573	36.3733	0.29820	2.4679	2.46801	9.96642	0.010067
		35.5174	0.34000	2.25409	2.52550	25.6458	0.001520

(AFM) Measurement

Surface morphology of Cu₂S films pure and doped %3 Bi were analyzed using AFM at (R.T and Ta=573 K). Figure 2 shows AFM images of Cu2S films in three dimensions (3D). These pictures indicate that all films are packed together and distributed in a uniform manner, with no pinholes or cracks. Table (3) shows AFM data; from this table, it can be determined that average grain size increased from (105.05) nm to (158.12) nm. After doping and annealing (at Ta=573 K), the toughness of film surfaces increased, and the root-mean square RMS surface changed due to structural enhancement, which agrees with X-ray diffraction results.

TABLE 3. Cu2S thin film AFM results

Thin Films	T_a (K)	Surfaces roughness (nm)	Root mean Sq.(nm)	Grain Size(nm)
Pure	R.T	5.93	7.16	105.05
	573	23.8	29.5	170.82
Cu₂S :3%Bi	R.T	4.16	5.18	158.12
	573	2.39	3.21	144.18

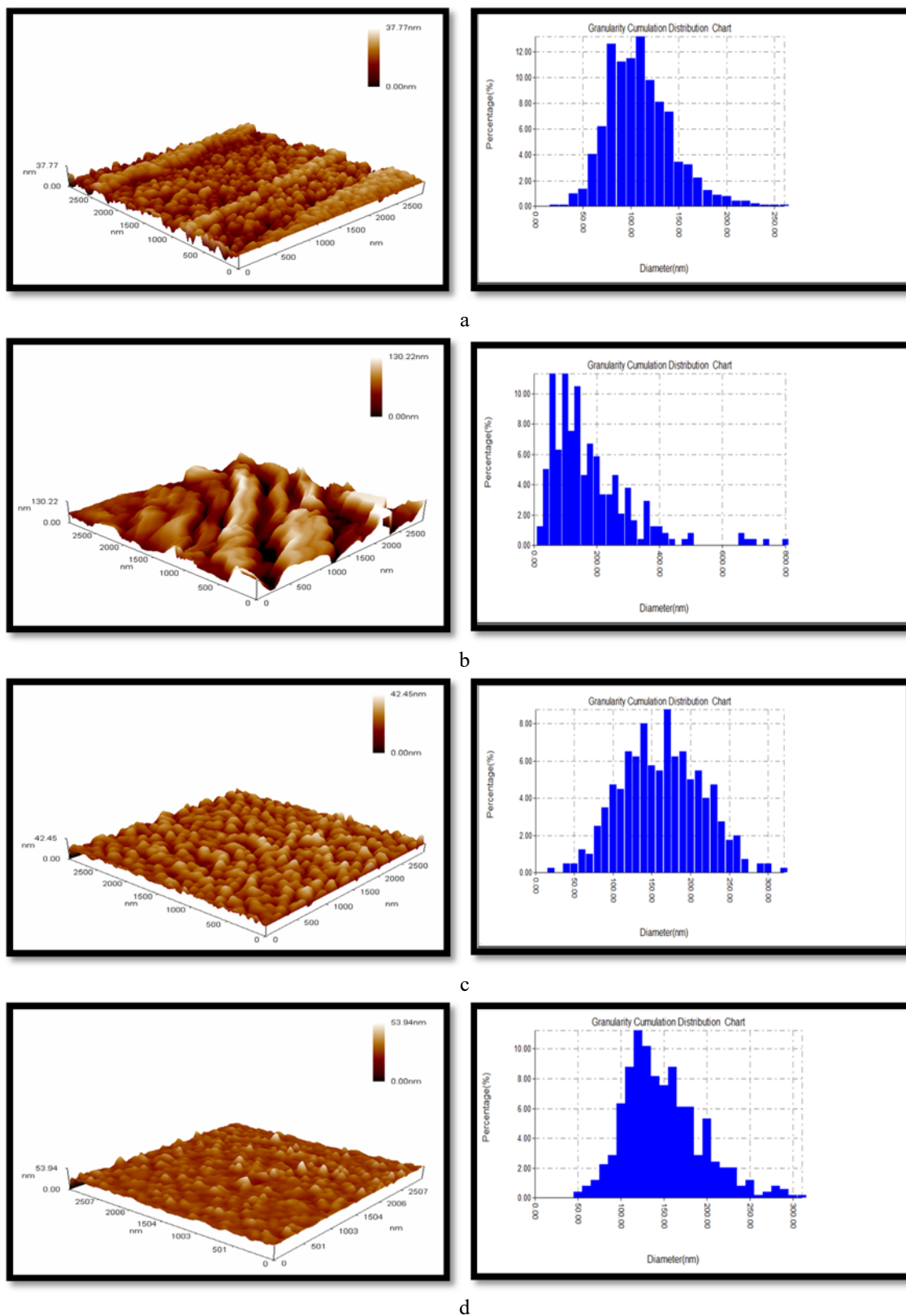**FIGURE 2.** AFM images of Cu₂S thin films. a) pure at R.T. b) pure at Ta=573 K. c) doped 3% Bi at (273k). d) doped 3%Bi at (Ta=573 K)

Optical Measurement

Figure 3 depicts the absorbance (A) as a function of wavelength limited extent (300 – 1000) nm for Cu_2S thin films pure and doped 3% Bi at (R.T and Ta=573 K) . This form shows how absorption values increase after doping and annealing due to a reduced cereal border and the creation of microscopic cereal, but decrease as wave length increases. Cu_2S films have a high absorption value across a wide wavelength range (400-600 nm), making them suitable for solar cell implementation. At (R.T and Ta=573 K), the permeability (T) of Cu_2S thin films pure and doped with % Bi is shown in Figure (4). The value of permeable increases with increasing wave length and high values in the NIR area, and increases after doping and annealing, this behavior relating to differences in crystal structure after doping and annealing is obvious from this form. As demonstrated in form (5)., all Cu_2S films have substantial absorption coefficients ($\alpha > 10^4$ cm^{-1}). This suggests that a direct transfer is likely to be permitted. In addition, the values of the absorption coefficient increase after doping, but the absorption coefficient is slightly reduced after annealing, resulting in a lower energy displacement, because absorption is not solely the responsibility of the freedom holders, but also of impurities or electronic states in a steady state.
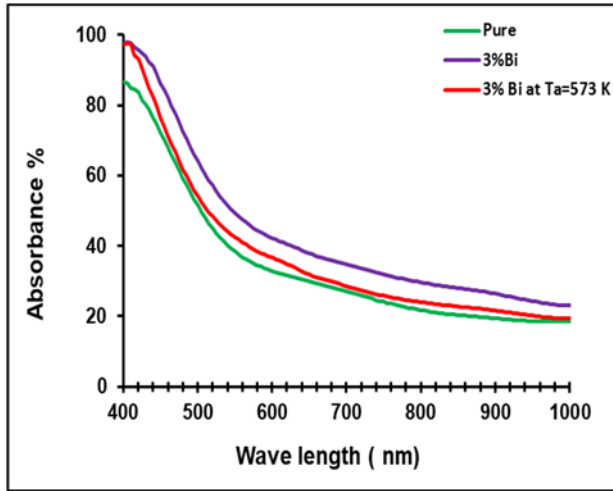

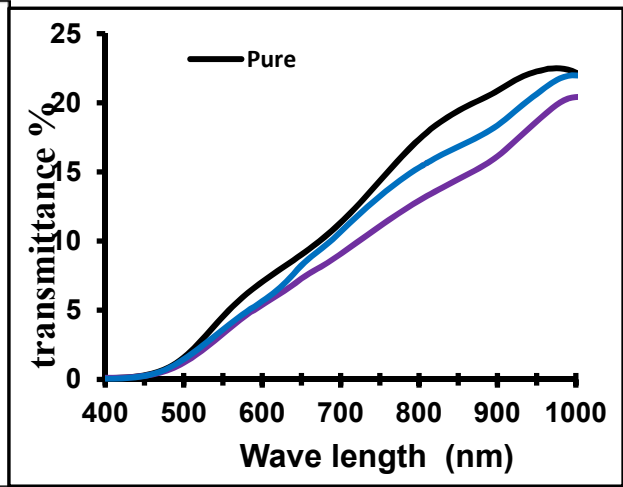**FIGURE 3.** Cu_2S thin film absorption as of wavelength.

FIGURE 4. The permeability of Cu_2S thin films as a function of a wavelengths.

The visual energy gap (Eg^{opt}) values determined from Tauc's equation are plotted $(\alpha h\nu)^2$ as a function of photon energy (hν) in Figure (6) :[24,25]

$$(\alpha h\nu) = A(h\nu - E_g)^n \quad \ldots\ldots\ldots(3)$$

Where A: is constant and n is a variable number based on the type of visual transition. After doping, the visible energy gap values of Cu2S thin films decreased from (2.25eV) to (2eV), but after annealing, the energy gap value increased to (2.2eV), indicating a red shift towards the absorption edge, as illustrated in Figures (6) and (7). Due to the difference in ionic radii, this behavior can be attributed to an increase in defects as a result of combining Cu+2 ions with Bi+3 ions. These values produce good material for solar cells.
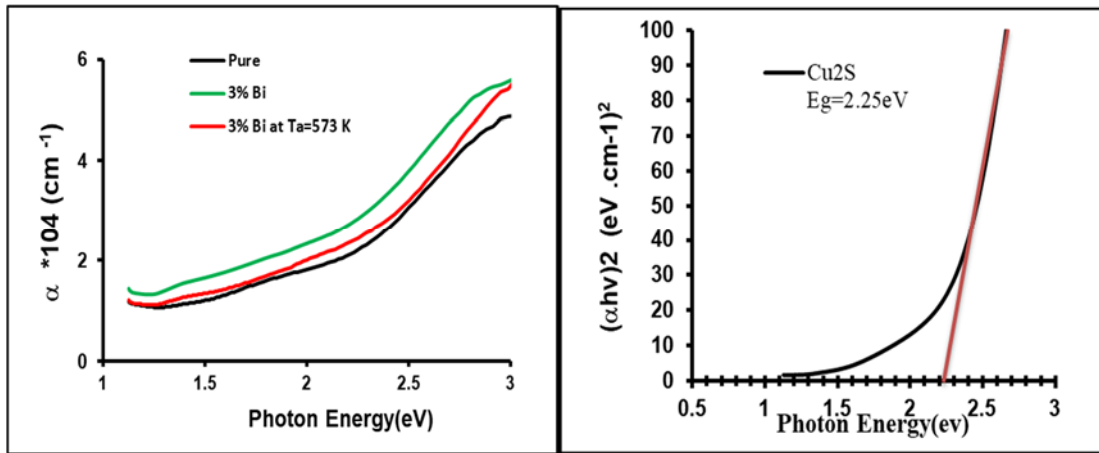
Figure 5. The relation between the absorption coefficient and photon (a) energy for Cu$_2$S thin films.
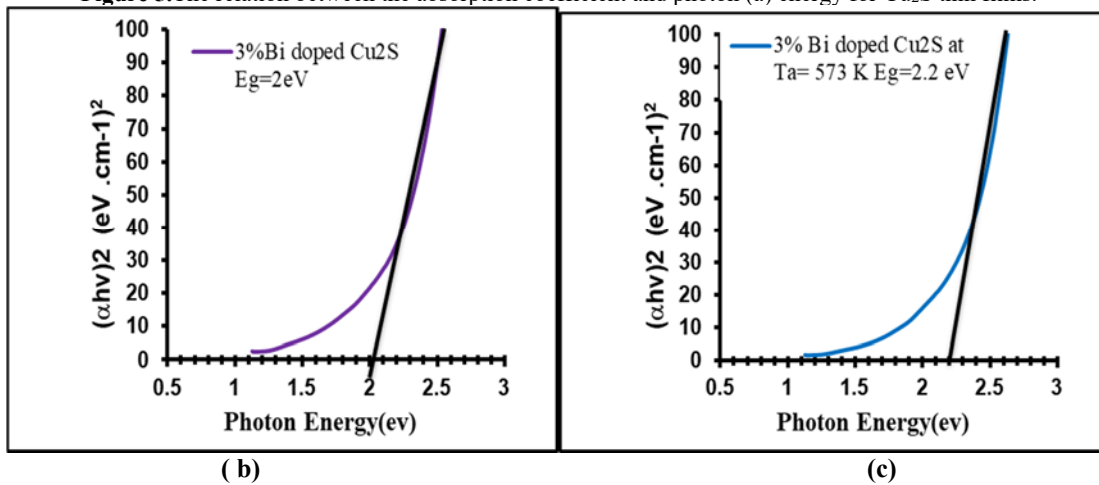

(b)   (c)

FIGURE 6. In Cu2S thin films, the connection between (αhv)2 and photon energy. a) pure at R.T. b) 3 % Bi (Cu2S) doped at R.T , b) 3% Bi doped at (Ta=573 K) .
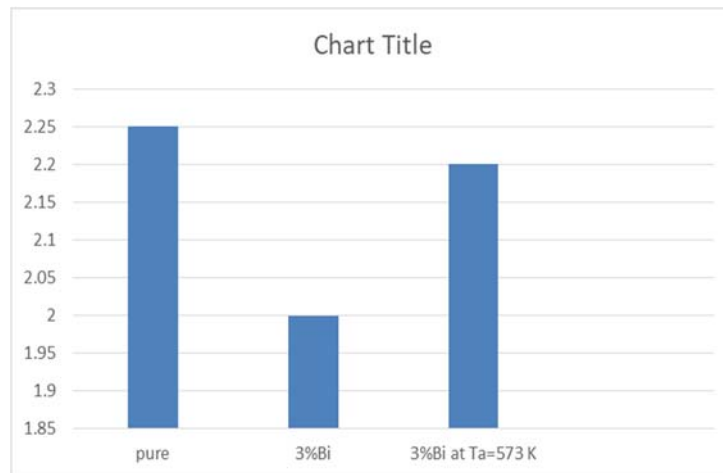

FIGURE 7. The optical energy gap for (Cu$_2$S and Cu$_2$S:3% Bi) films.

The formula can be used to compute refractive index values: [26]

$$n = \{[4R / (R-1)]-K^2\}^{1/2} - [(R+1) / (R-1)]\ldots\ldots\ldots\ldots\ldots.. (4)$$

R is the reflectance, which is computed using the following equation:

$$R = 1-T-A \quad \ldots\ldots\ldots\ldots\ldots\ldots\ldots\ldots\ldots.. \quad (5)$$

The absorption coefficient (α) and the extinction coefficient (K) are connected by: [27]

$$\alpha = 4\pi K / \lambda \quad \ldots\ldots\ldots\ldots\ldots\ldots\ldots\ldots \quad (6)$$

Figure 8 shows the behavior of the refractive index (n) with photon energy for (Cu_2S, Cu_2S:3 % Bi, and Cu_2S:3 % Bi at Ta=573 K) films. At increasing photon energy, refractive index values increase due to changes in the structural properties of films after doping and annealing. Figure (9) shows the fluctuation of the extinction coefficient (K) with photon energy for pure and doped % Bi Cu_2S thin films at (R.T and Ta=573 K), We can see from this graph that the extinction coefficient values increase after doping and annealing, and that this behavior is comparable to that of the absorption coefficients across the whole wavelength spectrum.
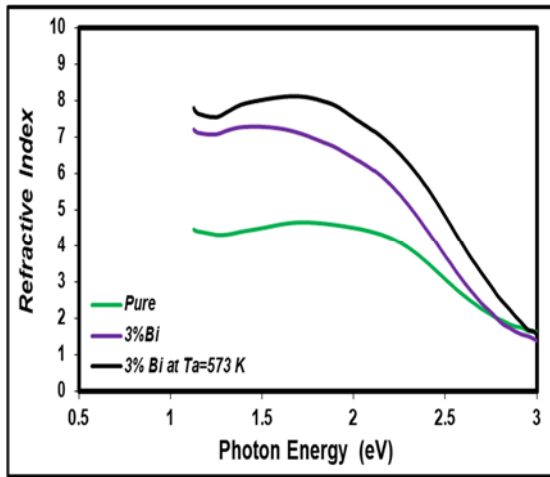

FIGURE 8. Variation of refractive index versus photon energy in Cu_2S thin films.
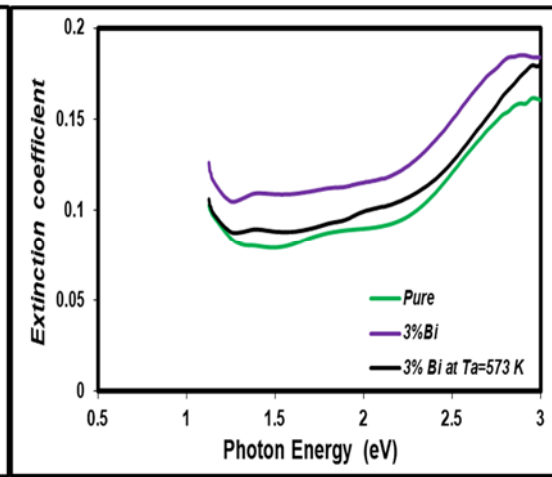
FIGURE 9. Extinction coefficient difference as a function of photon energy in Cu_2S thin films.

The real and imaginary parts of the dielectric constant (ϵ_1, ϵ_2) can be computed using the equation: [26].

$$\epsilon_1 = n^2 - K^2 \quad \ldots\ldots\ldots\ldots\ldots\ldots\ldots\ldots \quad (7)$$

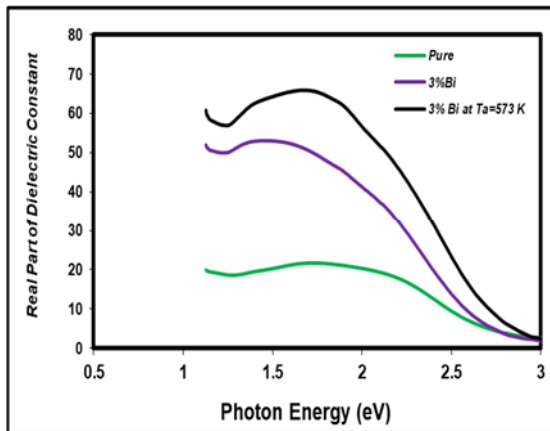$$\epsilon_2 = 2nK \quad \ldots\ldots\ldots\ldots\ldots\ldots\ldots\ldots \quad (8)$$

Figure 10 shows the difference of the real part of the dielectric constant versus photon energy in Cu_2S thin films.
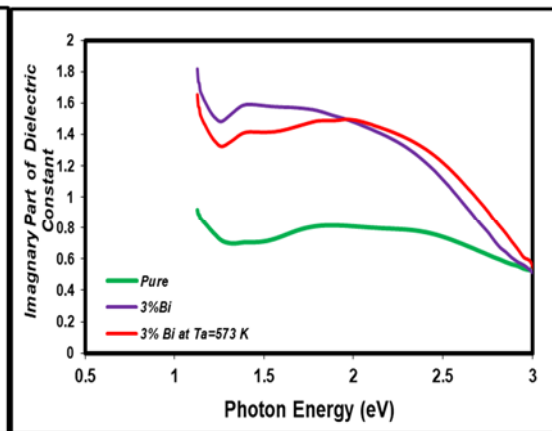
Figure 11 shows the difference of the imaginary part of the dielectric constant versus photon energy in Cu_2S thin films

The fluctuation of the real (Ɛ1) and imaginary (Ɛ2) components of the dielectric constant values vs photon energy for (Cu_2S, Cu2S:3% Bi, and Cu_2S:3% Bi at Ta=573 K) films is shown in Figures 10 and 11. The refractive index numbers determine the real component of the dielectric constant, whereas the extinction coefficient values determine the imaginary part of the dielectric constant.

CONCLUSION

XRD results show that the films were formed of Cu_2S phase and polycrystalline with preferential orientation in (220) direction in this study, which determines the influence of doping (3% Bi) and annealing temperatures on structural. Surface morphology and optical characteristics of Cu_2S thin films with a thickness of 400nm successfully produced on a glass substrate using the thermal evaporation process at R.T. The AFM results demonstrate that following 3% Bi doping and annealing temperature, both grain size and surface roughness altered. Increase grain size from 105.05 to 158.12 nm due to structure improvement and Low roughness can get good character for photovoltaic cell properties.Cu_2S films band gap energy values are depending on doping and annealing, decrease from 2.25 to 2 eV, lower values are obtained for Cu_2S:3% Bi with low transmittance. Films' optical properties indicate that they are suitable for photovoltaic applications.

REFERENCES

1. P.Sateesh, P. Madhusudhanarao, International Journal of Advanced Research in Physical Science (IJARPS), Volume 2, Issue 11, November 2015, PP 11-16
2. R. S. Patil, T.P. Gujar, C.D. Lokhande, R.S.Mane, Sung-Hwan Han, Journal of non-crystalline Solids, 353(2007).
3. S. Suresh, C. Raveendra Reddy, G. Suresh Babu, T. Veera Reddy, IJSDR Volume 1, Issue 9, 2016
4. Nair, P. K., and Nair, M. T. S.,, J. PHY., D, Appl.Phy. 1991, 24, 83-88.
5. Yamamoto, T., Kubota, E., Taniguchi, A., Dev, S., Tanaka, K., and Osakada, K., Chem.Mater. 1992, 4, 570-576
6. Nair, M. T. S, and Nair, P. K., Semicond.Sci.Technol., 1989,4,191-199.
7. Sagade, A. A., and Sharma, R., Sensors and Actuators B: Chemical, 2008, 133, 135-143.
8. Pathan, H. M., Desai, J. D., and Lokhande, C. D, Appl. Surf. Sci., 2002,202, 47-56.
9. M. Ramya, and S. Ganesan, Iranian Journal of Materials Science & Engineering Vol. 8, Number 2, Spring 2011
10. P.J Sebastian, O. Gomez-Daza, J. Campos, L Banos, and P.K. Nair, Sol. Energ. Matter. Sol. C.32 (1994)159.
11. S. Lindross, A Arnold and M Leskela, Appl. Surf. Sci. 158 (2000) 75.
12. F. Li, T. Kong, W.T.Bi, D.C.Li, and X.T. Huang, Appl. Surf. Sci. 255 (2009) 6285.
13. J. Liu and D.F. Xue, J.cryst. Growth, 311 (2009) 500.
14. Y.-J. Wang, A.-T. Tsai, C.-S. Yang, Mater. Lett. **63**, 847(2009).
15. S.V. Bagul, S.D. Chavhan, R. Sharma, J. Phys. Chem. Solids, **68**, 1623(2007).
16. S.G. Chen, Y.F. Huang, Y.Q. Liu, Q. Xia, H.W. Liao, C.G. Long, Mater Lett., **62**, 2503(2008).
17. S. Bini, K. Bindu, M. Lakshmi, C. SudhaKartha, K.P. Vijayakumar, Y. Kashiwaba, T. Abe, Renewable Energy , **20**, 405(2000).
18. C.G. Munce, G.K. Parker, S.A. Holt, G.A. Hope, A. Colloids Surf. **295**, 152(2007).
19. L. Isac, A. Duta, A. Kriza, S. Manolache, M. Nanu, Thin Solid Films, **515**, 5755(2007).
20. X. B. He, A. Polity, D. I. Osterreicher, D. Pfisterer, R. Gregor, B. K. Meyer and M. Hard, Physica B: Condensed Matter, **308**, 1069(2001).
21. MudiXin, KunWei Li, Hao Wang, Applied Surface Science, **15**, 1436(2009).
22. S. Schneider, J.R. Ireland, M.C. Hersam, T.J. Marks, Chem. Mater., **19**, 2780(2007).
23. Ghuzlan Sarhan Ahmed, and Bushra K. H. Al-Maiyaly, AIP Conference Proceedings **2123**, 020074 (2019)
24. Bushra H. Hussein, Hanan K. Hassun, NeuroQuantology **18**(5), 77 (2020).
25. B. K. H. AL-Maiyal, B. H. Hussein and H. K. Hassun, Journal of Ovonic Research, **16** (5), (2020).
26. B. K. H. AL-Maiyal , Ibn Al-Haitham J. for Pure & Appl. Sci vol.26,(1) 2013
27. B. K. H. AL-Maiyal , Ibn Al-Haitham J. for Pure & Appl. Sci, Vol. 28 (3) 2015